Improved photon harvesting by employing C_{70} in bulk heterojunction solar cells

Steffen Pfuetzner[a], Jan Meiss[a], Selina Olthof[a], Moritz P. Hein[a], Annette Petrich[a], Lothar Dunsch[b], Karl Leo[a], and Moritz Riede[a]

[a] Institut für Angewandte Photophysik, Technische Universität Dresden, George-Bähr-Straße 1, 01069 Dresden, Germany, http://www.iapp.de;

[b] Leibniz-Institut für Festkörper- und Werkstoffforschung Dresden, Helmholtzstraße 20, 01069 Dresden, Germany

ABSTRACT

To achieve higher efficiencies in organic solar cells, ideally the open circuit voltage (V_{OC}), fill factor (FF) as well as the short current density (J_{SC}) have to be further improved. However, only a few suitable acceptor molecules, e.g. C_{60}, are currently available for the photoactive layer. Despite a good electron mobility on the order of 1×10^{-3} cm^2/Vs the absorption of C_{60} in the visible sun spectrum is low. From polymer based solar cells it is known that the fullerene derivative [70]PCBM used in the photoactive layer shows a significant enhancement in J_{SC} compared to [60]PCBM. This work investigates the application of fullerene C_{70} as acceptor in comparison to the well known C_{60} in vacuum processed small molecule solar cells. C_{70} shows a broadened and red shifted absorption (abs. maximum around 500 nm) compared to C_{60}. By fabricating p-i-i solar cells we show that the stronger absorption of C_{70} leads to enhanced photon harvesting and increased external quantum efficiency. The bulk heterojunction p-i-i solar cell containing C_{70} as acceptor and ZnPc as donor, co-evaporated with an optimized ratio of 2:1, and a layer thickness of 30 nm shows improved solar cell parameters: a 30% larger photocurrent of 10.1 mA/cm^2 is obtained. The V_{OC} of 0.56 V and FF of 55% remain comparable to C_{60}-containing p-i-i solar cells. Therefore, the solar cell performance is mainly improved by J_{SC} and leads to a mismatch corrected power conversion efficiency of 3.12%. Thus, we show that C_{70} is an alternative fullerene to C_{60} for solar cell applications.

Keywords: organic solar cell, small molecule, fullerene, C60, C70, bulk heterojunction, p-i-i, p-i-n,

1. INTRODUCTION

Contrary to fossil fuels, solar energy represents an inexhaustible energy source. An elegant approach to directly generate electric energy using the photovoltaic effect, where silicon solar cells are well established. An alternative arises with the field of organic solar cells, which have the potential for low production costs (e.g. screen printing,[1] vacuum deposition, roll to roll production, spin coating etc.). Organic dyes with high absorption coefficients lead to thin active layers (< 100nm) and allow for flexible devices.[2] Therefore innovative solar cell applications are possible (e.g. in architecture and automobile industries).
The first flat heterojunction organic solar cells with a power conversion efficiency of approximately 1% were made by Ching Tang[3] in 1986. Good progress has been made since then, but it is still a challenge to obtain high power conversion efficiencies and flexible encapsulation.[4]

The organic solar cells in this paper are based on the p-i-n concept.[5,6] This means that the intrinsic active absorbing part (i) is sandwiched between doped transport layers for electrons (n) and holes (p), respectively, as sketched in Fig. 1(a). The controlled doping of the transport layers[7,8] leads to high conductivities and ensures loss-free transport of electrons and holes towards the electrodes, respectively. The wide gap materials used

Further author information: (Send correspondence to S.P.)
S.P.: E-mail: steffen.pfuetzner@iapp.de, Telephone: +49(0)351 46338773
M.R.: E-mail: moritz.riede@iapp.de

Photonics for Solar Energy Systems III, edited by Ralf B. Wehrspohn, Andreas Gombert, Proc. of SPIE
Vol. 7725, 77250E · © 2010 SPIE · CCC code: 0277-786X/10/$18 · doi: 10.1117/12.854402

as transport materials are furthermore excellent charge-carrier (for opposite charges) and exciton blocker,[9] as schematically shown in Fig. 1(b).
The power conversion efficiency (η_{eff}) of a solar cell is defined as follows:

$$\eta_{eff} = \frac{J_{\mathrm{SC}} \times V_{\mathrm{OC}} \times FF}{I_0}. \quad (1)$$

Where J_{SC} is the photocurrent density, V_{OC} the open circuit voltage, and FF the fill factor. I_0 refers to the intensity of the irradiance light. Usually a standard AM1.5 G (Air Mass) sun spectrum with 100 mW/cm^2 total power density is used for sample illumination.[10]
To obtain higher power conversion efficiency, further optimisation of different parts of a solar cell has to be carried out: the photovoltaic active part: (a) open circuit voltage V_{OC}, (b) photocurrent density J_{SC} (photon absorption), and (c) transport properties reflected in the FF (e.g. mobility); secondly the transport layers: (a) conductivity, (b) mobility, (c) thermal and morphological stability, (d) transparency in the absorption region of the photoactive absorber system, and (e) compatible energy level alignment to the neighboring photoactive layers.

Since organic solar cells are thin film devices and standing waves are formed due to the highly reflective metal back contact, the optical field distribution can be optimised to the stack position of the photoactive absorber layer.[11] This can be achieved by varying the thicknesses of the transparent n/p-transport layers.
To avoid peformance losses due to transport of the charge carriers, the hole and electron transport materials have to fulfil the requirements mentioned above. A study concerning hole transport materials was recently done by Pfuetzner et al.[12] In this work we focus on the photoactive absorber layers, in particular on photocurrent enhancement. It is well known from the polymer solar cells that [70]PCBM provides higher photocurrents compared to [60]PCBM.[13] We investigate in this work the pure fullerene C_{70} and compare it with the well known standard acceptor molecule C_{60}.[14] The characterisation is made in particular for absorption properties, electron mobility, ultraviolet photoelectron spectroscopy (UPS), and application in bulk heterojunction organic solar cells.

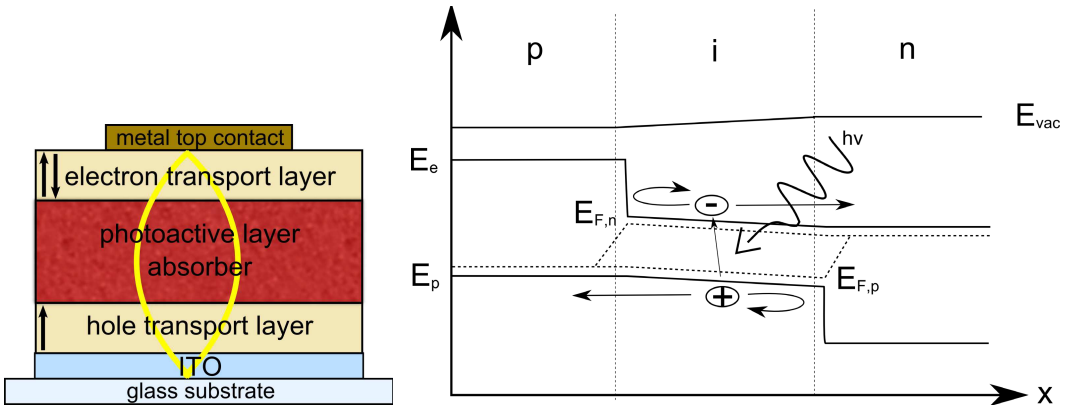

(a) (b)

Figure 1. (a) Stack of a p-i-n solar cell: the p- and n- transport layers can be varied for optimised field distribution. The incident light (black arrows) forms a standing wave (yellow) due to the highly reflective metall contact. (b) Energetic diagram of an ideal p-i-n solar cell: doped materials with wide band gaps form the p- and n- like regions. The transport layers behave like selective membranes due to the large gap to the intrinsic material.

2. EXPERIMENTAL

Materials. The organic materials C_{60} (Bucky USA) and zinc phthalocyanine (ZnPc (Alpha Aesar,VWR, and TCI)) are used as reference and standard photoactive absorber system to investigate new materials.
For the initial tests high quality C_{70} are kindly provided by IFW[b]. Further larger amounts of C_{70} for systematic

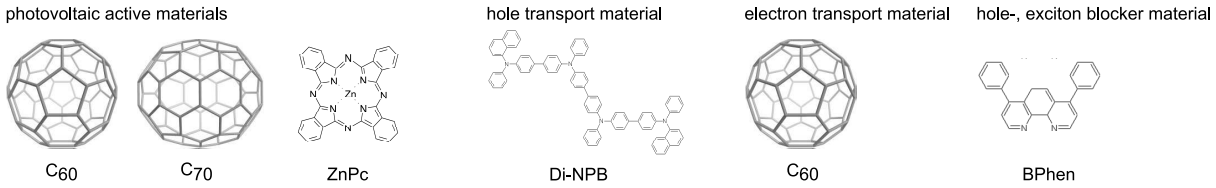

Figure 2. Molecular structures of: standard photoactive materials C_{60} and ZnPc; investigated fullerene C_{70}; hole transport materials Di-NPB; exciton and electron blocking material BPhen.

investigations are purchased from Bucky USA in a purity of 99.0%
N,N'-diphenyl-N,N'-bis(4'-[N,N-bis(naphth-1-yl)-amino]-biphenyl-4-yl)-benzidine (Di-NPB, Sensient GmbH) is used as hole transport material. For controlled doping of the hole transport layer, the p-dopant NDP2 (Novaled AG, Dresden) is used instead of the 2,3,5,6-tetrafluoro-7,7,8,8-tetracyanoquinodimethan (F_4-TCNQ) due to the better processability. Comparative experiments show that the electronic properties of doped layers are similar for both dopants.[15]
Before use, all materials are purified at least twice by vacuum gradient sublimation to improve material purity and minimise trap states.[16] Molecular structures of the materials are shown in Fig. 2.

Preparation and Characterisation

The investigated organic solar cells are fabricated in a custom-made vacuum system (K.J. Lesker, U.K.) at a base pressure of 1×10^{-8} mbar, using shadow masks. Glass substrates with coated and prestructured ITO (30 $\frac{\Omega}{\text{sq.}}$) (Thin Film Devices Inc.) precleaned with acetone and ethanol and pretreated in oxygen plasma is used as substrate. 16 samples are made on the same wafer in one run, ensuring reproducible and comparable conditions for all layers. Quartz glass is used for optical investigations.
The thermal deposition rate of organics is set to be between 0.2 - 0.5 Å/s at ambient conditions. The doped transport materials (matrix and dopant) and the photoactive absorber materials (C_{60}, C_{70}, and ZnPc) are co-deposited. The deposition rate of each source is controlled by a oscillating crystal and monitored (Leybold Inficon Inc. Deposition Monitor XTM/2). To prevent degradation, all devices are encapsulated in a glovebox with nitrogen atmosphere. Current density - voltage (J-V) characteristics are recorded using a source measurement unit 236 SMU (Keithley) under an AM 1.5 G sun simulator, monitored with a Hamamatsu S1337 silicon photodiode with respect to which intensities are measured. Spectral mismatch between the simulated and the AM 1.5 G sun spectrum or between the spectral response of reference cell and test cell is taken into account.
The active area of the devices is defined by the overlap of the electrodes indium-tin-oxide (ITO) and the top metal contact and is about 6.7 mm^2 (measured by a light microscope).
External quantum efficiency (EQE) is measured employing lock-in techniques (Signal Recovery SR 7265 lock-in amplifier) in a custom-made setup with Xe illumination and a Newport Oriel Apex monochromator illuminator. The samples are measured through a photomask having an aperture of 2.958 mm^2. The absorption spectra of 20 nm neat fullerene layers, deposited on quartz glass, are analysed by spectrometer (Shimadzu MPC-3100). The measurements are carried out ex-situ under ambient conditions.
The mass spectra are measured using a Biflex MALDI-TOF spectrometer (Bruker Daltonic). Excitation is performed at 337 nm using a N2 laser. Both methods, relative to a negative and positive electrode are carried out, but only the results relativ to the negative electrode are shown here due to similar results.
Organic field effect transistors (OFETs) are used here for electron mobility determination. The OFETs typically consist of a silicon gate and silicon oxide. The OFET substrates with prestructured source and drain Au contacts and a channel length in the range of 2.5 μm-20 μm are purchased from the Fraunhofer IPMS (Dresden). C_{60} and C_{70} layers of 20 nm are deposited on the OFET substrates. Current density - voltage (J-V) characteristics are recorded using source measurement units 236 SMU (Keithley).
Ultraviolet photoelectron spectroscopy (UPS) measurements to determine the ionisation potential (IP) of the fullerenes are performed with a Phoibos100 system (Specs, Berlin, Germany) under ultrahigh vacuum (UHV) with a base pressure of 1×10^{-10} mbar. For UPS measurements, the He I line (21.22 eV) from a discharge lamp with an energy resolution of 130 meV and for x-ray photoelectron spectroscopy (XPS) an Al K_α x-ray source (1486.6 eV) with a resolution of 400 meV are used. The experimental error of both methods can be estimated

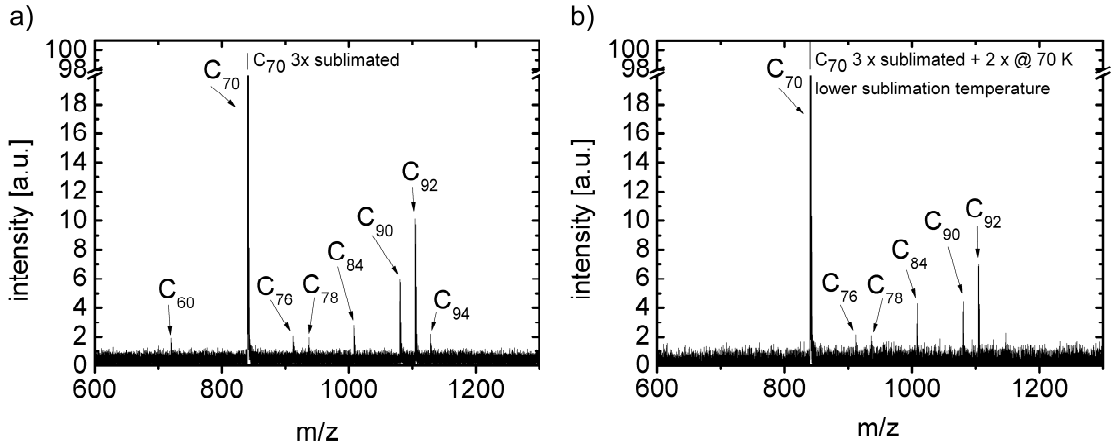

Figure 3. Mass spectroscopy measurements of a) 3x sublimated C_{70} soot show presence of high ordered fullerenes b) additionally 2x sublimated soot at 70 K lower sublimation temperature show reduced amounts of higher numbered fullerenes, C_{60} and C_{94} disappear, for C_{76} and C_{78} no signal is seen, while C_{84}, C_{90}, and C_{92} remain in smaller amounts.

from the reproducibility achieved in separate measurements and is below 50 meV. The Bestec UHV evaporation tool with a base pressure of 1×10^{-8} mbar for the deposition of the organic layers is directly connected to the measurement chamber and different chambers for n- and p-type doping as well as for intrinsic layers can be used to avoid cross contamination.

3. RESULTS

3.1 Characterisation of the fullerene C_{70}

3.1.1 Mass spectroscopy

For fullerene production a generator on the basis of the Krätschmer-Huffman method is used. Due to the production procedure of C_{70} other fullerenes (e.g. C_{60}, C_{84}...) can be present in the nominal purity of 99.0% C_{70} soot, which might act as traps for charge carriers and negatively influence the device performance. Therefore, the C_{70} is sublimated to minimise the impurities as much as possible. To ensure the quality and purity of the C_{70} soot mass spectrum measurements are carried out.

The mass spectrum of the three times sublimated C_{70} Fig. 3a) shows the presence of various higher numbered fullerenes, which can be indentified (molecular weight in brackets) as C_{76}[912.84], C_{78}[936.86], C_{84}[1008.92], C_{90}[1080.99], C_{92}[1105,01], and C_{94}[1129.03]. Even C_{60}[720.66] is present.

To minimise the amount of impurities (higher numbered fullerenes), the C_{70} soot is sublimated once more at 70 K lower sublimation temperature for two times. In the mass spectrum (Fig. 3b)) a reduction of the fullerenes derivatives can be seen. The peaks for fullerenes C_{60} and C_{94} disappeared completely. For C_{76} and C_{78} no signal is seen. However, below a certain signal it is not really possible to distinguish here between a fullerene signal and background noise. Just little amounts of C_{84}, C_{90}, and C_{92} remain. Please note: The intensity peaks do not correlate to relative frequencies, due to a different ionisability of the elements, but they are comparable with each other. The improved C_{70} purity by resublimation is checked in solar cell devices and is confirmed by J-V measurements of bulk heterojunction solar cells containing purified C_{70} and discussed in section 3.2.

3.1.2 Optical properties

20 nm of pure C_{60} and C_{70} are deposited seperately on quartz glass, and investigated spectroscopically. From the absorption measurements (Fig. 4) it can be seen that C_{70} shows a stronger absorption in the visible range of light from 380-800 nm. A broad absorption maximum is determined at 515 nm for C_{70}. Futhermore, the absorption onset is around 705 nm for both materials (shown in the inset of Graph 4) and hints at similar optical

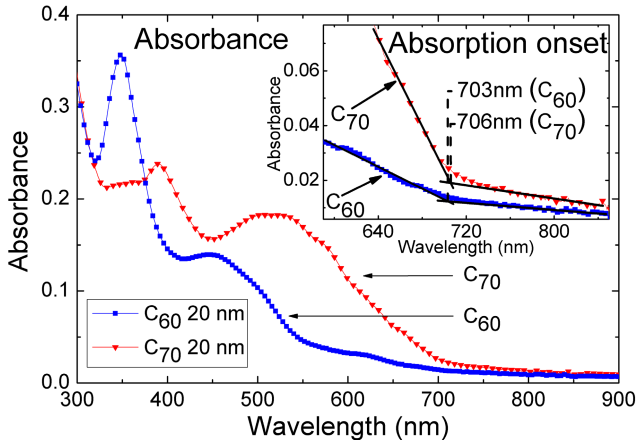

Figure 4. Absorption measurements of 20 nm C_{60} (filled squares) and C_{70} (filled up side down triangles), C_{70} shows a broadened and stronger absorption in the visible range of light compared to C_{60}. Inset: Fit of the absorption onset of C_{60} and C_{70}, and determined for both at around 705 nm.

gaps of around 1.75 eV. The optical bandgap is calculated as follows:

$$E_G^{opt} = \frac{hc}{\lambda_{onset}} \tag{2}$$

(3)

Different absorption behaviour is observed, but the optical band gaps are similar for both, C_{60} and C_{70}. That is caused by transitions which are forbidden in C_{60} due to the high molecular symmetry and allowed for the ellipsoid shaped C_{70}.[17] C_{70} shows a higher absorption compared to C_{60}. To check if the enhanced photon absorption can efficiently be used by converting the absorbed photons into free charge carriers bulk heterojunction solar cells are processed and discussed in section 3.2.

3.1.3 Ultraviolet photoelectron spectroscopy (UPS)

To determine the ionisation potential (IP) levels of the fullerene layers, 10 nm of C_{60} and 15 nm of C_{70} are deposited on a 0.5 mm thick silver foil, respectively.
The IP can be calculated by the measured values of hole injection barrier (HIB), high binding energy cutoff (HBEC) and the given engery of the discharge lamp (21.22 eV) as follows:

$$\mathrm{IP} = 21.22\mathrm{eV} - \mathrm{HBEC} + \mathrm{HIB} \tag{4}$$

The HBEC and HIB, see Fig. 5, are determined at 16.55 eV and 1.74 eV for C_{60} and 16.72 eV and 1.91 eV for C_{70}, respectively. This leads to a similar IP of -6.41 eV for C_{60} and C_{70}.
Since the electron affinities (EA) of C_{60}[18] and C_{70} both appear at -4.0 eV, no significant difference in V_{OC} is expected in m-i-p bulk hetero junction solar cells, which is confirmed by the same V_{OC}=0.56 V.[19] The obtained IP of C_{70} at -6.41 eV provides an energy offset of at least 1.13 eV to the IP of ZnPc (-5.0 eV to -5.28 eV[20,21]), which is larger than the exciton binding energy of C_{70} and large enaough to get an efficient exciton dissociation.[22]

3.1.4 Mobility measurements

To ensure high V_{OC} and efficient charge carrier extraction out of the bulk layer and reduce, charge carrier mobilities of both, electrons and holes should be in the range of 10^{-3} cm^2/Vs to 10^{-6} cm^2/Vs. Therefore, mobility measurements for the acceptor-like fullerenes are carried out. Usually, in organic solar cells, charge carriers move perpendicular to the substrate, while in OFET the mobility of the charge carriers is measured

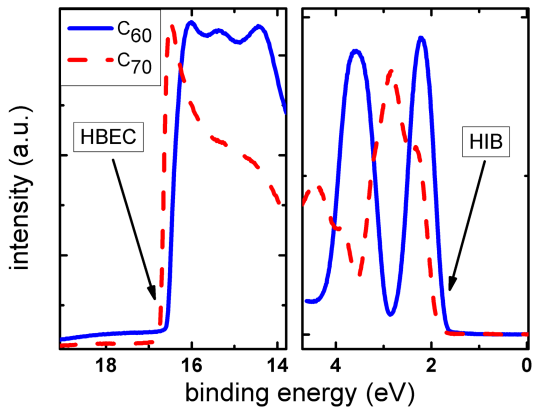

Figure 5. UPS measurement of 10 nm C_{60} (solid line) and 15 nm C_{70} (dashed line) on silver foil, respectively. The left graph shows the high binding energy cutoff (HBEC) and the righ graph the hole injection barrier for both fullerenes.

parallel to the substrate. Due to the fact that C_{60} and C_{70} are symmetric and shaped like a ball or an ellipsoid, no preferential molecular arrangement is predominant. Therefore, using the OFET method, no significant deviations in mobilities are expected.
Substrates are evaporated with either 50 nm thick C_{60} and C_{70} layers and characterised electronically. The electron mobility (μ_e) can be determined from both linear and saturation regime of the J-V characteristics, in Fig. 6a) shown for the C_{60} OFET J-V characteristic by varying U_G from 10.4 V to 23.8 V. From equation (5), corresponding to the linear regime, the mobility is calculated by differentiation with respect to gate- and source-drain voltage, respectively. From the saturation regime, the mobility can be determined by using equation (6).

$$I_{SD} = \frac{C_i W}{L} \mu_e \left(U_G - U_{TH} - \frac{U_{SD}}{2} \right) U_{SD} \tag{5}$$

$$I_{SD} = \frac{C_i W}{2L} \mu_e (U_G - U_{TH})^2, \tag{6}$$

where I_{SD} is the current and U_{SD} the voltage measured between source and drain, U_G the gate voltage, L is the channel length of the transistor, W channel width, C_i capacitance per area of the oxide, and U_{TH}.
In the saturation regime μ_e can be determined by plotting $\sqrt{I_{SD}}$ versus U_G and fitting the linear part. When the threshold voltage (U_G) is large enough to generate a adequate charge carrier accumulation at the semiconductor-insulator-interface the slope in the plot becomes linear, see Graph 6b).

For these measurements OFETs with a channel width of 10 mm and a channel length of 20 μm for C_{60} and 2.5 μm for C_{70} are used.
The calculated μ_e from the linear regime as well as the fitted μ_e from saturation regime are shown in Tab. 1. The obtained mobilities for both linear and saturation regime differ slightly, but show μ_e in the order of 10^{-3} cm^2/Vs. Comparing C_{60} and C_{70}, similar mobilities are determined, which hints at comparable charge carrier transport properties.

3.2 p-i-i fullerene:ZnPc bulk heterojunction solar cells

The high absorption and electron mobility, as well as the estimated EA of C_{70} by flat heterojunction solar cells[19] are promising parameters to implement C_{70} in a bulk heterojunction solar cell.
The processed p-i-i solar cells have the following structure:

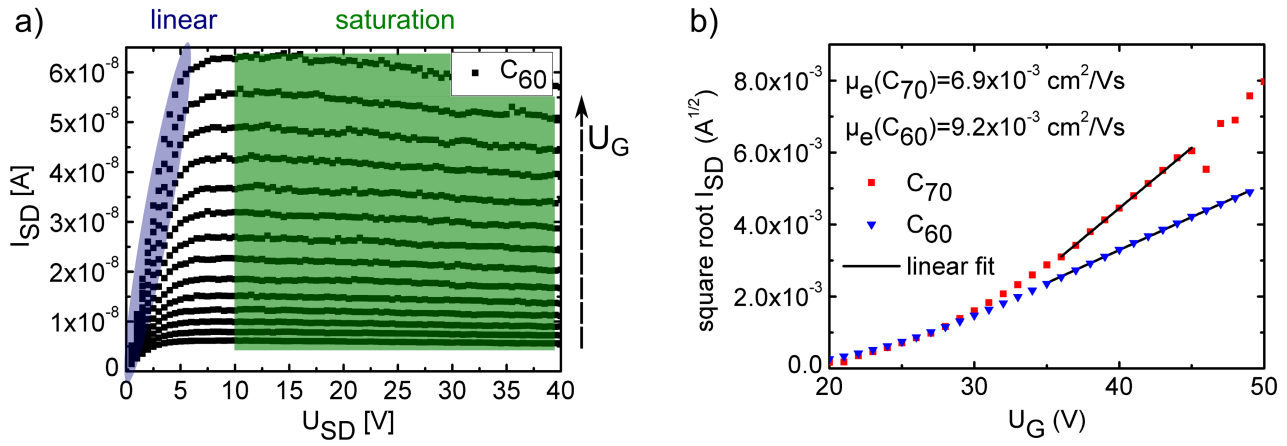

Figure 6. a) J-V mobility characteristic is shown for C_{60} by varying U_G from 10.4-23.8 V, the elctron mobility can determined in the linear (ellipse) as well as in the saturation regime (rectangle); b) plotting the square root of I_{SD} versus U_G of the saturation regime, the mobility can be determined by a linear fit for C_{60} data (filled up side down triangles) and C_{70} data (filled squares).

Table 1. Electron mobilities of C_{60} and C_{70} determined in the linear and saturation regime by OFET mobility measurements.

	$\mathbf{C_{60}}$	$\mathbf{C_{70}}$
μ_e linear regime [cm^2/Vs]	3.4×10^{-3}	2.0×10^{-3}
μ_e saturation regime [cm^2/Vs]	9.2×10^{-3}	6.9×10^{-3}

ITO/NDP2(1nm)/p-Di-NPB(60 nm; 5wt%)/C_{X0}:ZnPc(2:1; 30 nm)/C_{60}(40 nm)/BPhen(6 nm)/Al

The stack is optimised for the optical field distribution. Furthermore, the volume ratio for C_{X0}:ZnPc is determined to 2:1 as optimum for this absorber system. Only a little trend for C_{60}:ZnPc to ratio 1:1 is noted, while C_{70}:ZnPc tend to ratio 3:1, due to an assumed favourable molecular arrangement. The J-V characteristics are shown in Fig. 7 a) and the corresponding solar cell parameters are shown in Tab. 2. The J_{SC} is enhanced by over 35% by replacing C_{60} by C_{70} in the bulk heterojunction solar cell. That means the harvested photons are efficiently converted into free charge carriers and contribute to the photocurrent. This can also be proven by EQE measurements shown in Fig. 7b).

The absorption gap which is present in the C_{60}:ZnPc solar cell between 400-550 nm is almost filled by the C_{70} absorption. The V_{OC} and the *FF* are comparable for both devices.

Concluding from the solar cell results, it seems that the residual high numbered fullerenes in the C_{70} soot observed in mass spectra do not have any negative influence on the solar cell performance like trap states, etc.

No difference of the solar cell parameter V_{OC} and *FF* is observed, only improvement in J_{SC} is obtained. Therefore, C_{70} is a suitable acceptor molecule to replace C_{60} in organic solar cells.

Table 2. J-V characteristics of C_{X0}:ZnPc(2:1; 30 nm) bulk heterojunction solar cells containing C_{60} and C_{70}, respectively.

	V_{OC} [V]	J_{SC} [mA/cm^2]	*FF* [%]	S [$J_{SC}/J(-1V)$]	p.c. eff. [%]
C_{60}:ZnPc (2:1)	0.59	7.44	55.9	1.11	2.45
C_{70}:ZnPc (2:1)	0.55	10.1	56.1	1.13	3.12

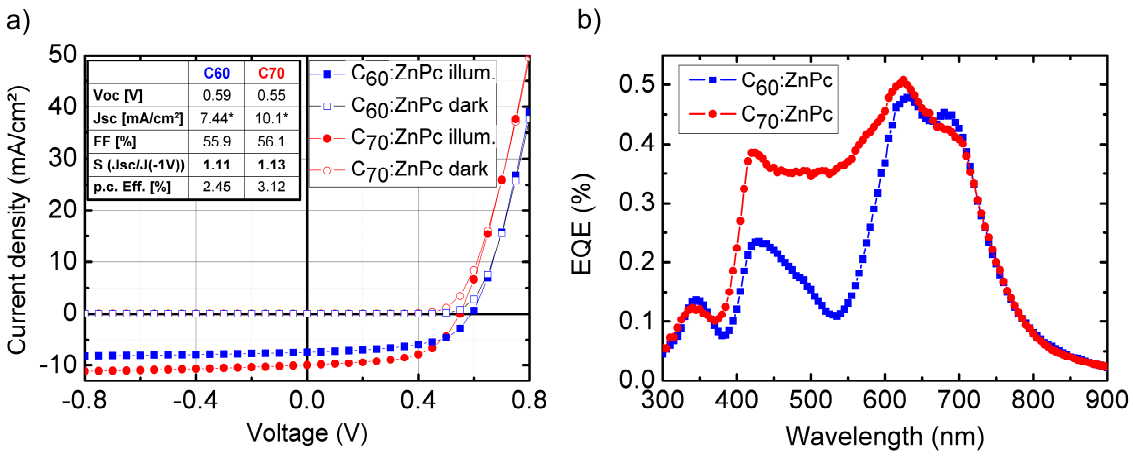

Figure 7. Bulk heterojuntion C_{60}:ZnPc and C_{70}:ZnPc solar cells with the following device structures are processed: ITO/NDP2(1nm)/p-Di-NPB(60nm;5wt%)/C_{X0}:ZnPc(2:1;30nm)/C_{60}(40nm)/BPhen(6nm)/Al. a) J-V characteristics: shown is C_{70} containing device at AM 1.5 G illumination (filled circles), in the dark (empty circles), and C_{60} containing device at AM 1.5 G illumination (filled squares) and in the dark (empty squares). The photocurrents are corrected for spectral mismatch and normalised to 100 mW/cm^2. b) EQE measurements of bulk heterojunction containing C_{70} (filled circles) and C_{60} (empty circles).

4. CONCLUSION

In this work, we have shown that the broader absorption of C_{70} compared to C_{60} leads to a significant increase of photocurrent in a C_{70}:ZnPc bulk heterojunction solar cell, despite the same optical band gaps of 1.75 eV. UPS measurements point out that C_{60} and C_{70} have similar IPs at -6.41 eV and enable due to large energy offset to the ZnPc IP an efficient exciton dissociation. Mobilities determined from the linear and saturation regime are in the order of 10^{-3} cm^2/Vs. Bulk heterojunction solar cells containing C_{70} are processed and show improved photocurrent contribution while V_{OC} and *FF* remain constant in comparison to C_{60}:ZnPc solar cells. Thus, we show that C_{70} is an alternative fullerene to replace C_{60} for solar cell applications.

ACKNOWLEDGMENTS

This work is supported by the Bundesministerium für Bildung und Forschung in the framework of the OPEG-project (13N9720 0204).

REFERENCES

[1] S. Shaheen, R. Radspinner, N. Peyghambarian, and G. Jabbour, "Fabrication of bulk heterojunction plastic solar cells by screen printing," *Applied Physics Letters* **79**, p. 2996, 2001.

[2] C. Lungenschmied, G. Dennler, H. Neugebauer, S. N. Sariciftci, M. Glatthaar, T. Meyer, and A. Meyer, "Flexible, long-lived, large-area, organic solar cells," *Solar Energy Materials And Solar Cells* **91**, p. 379, 2007.

[3] C. Tang, "Two-layer organic photovoltaic cell," *Applied Physics Letters* **48**, p. 183, 1986.

[4] G. Dennler, C. Lungenschmied, H. Neugebauer, N. S. Sariciftci, M. Latreche, G. Czeremuszkin, and M. R. Wertheimer, "A new encapsulation solution for flexible organic solar cells," *Thin Solid Films* **511**, p. 349, 2006.

[5] K. Walzer, B. Maennig, M. Pfeiffer, and K. Leo, "Highly efficient organic devices based on electrically doped transport layers," *Chemical Reviews* **107**, p. 1233, 2007.

[6] J. Drechsel, B. Maennig, F. Kozlowski, D. Gebeyehu, A. Werner, M. Koch, K. Leo, and M. Pfeiffer, "High efficiency organic solar cells based on single or multiple pin structures," *Thin Solid Films* **451-452**, p. 515, 2004.

[7] M. Pfeiffer, A. Beyer, T. Fritz, and K. Leo, "Controlled doping of phthalocyanine layers by cosublimation with acceptor molecules: A systematic seebeck and conductivity study," *Applied Physics Letters* **73**, p. 3202, 1998.

[8] B. Maennig, M. Pfeiffer, A. Nollau, X. Zhou, P. Simon, and K. Leo, "Controlled p-doping of polycrystalline and amorphous organic layers: Self-consistent description of conductivity and field-effect mobility by a microscopic percolation model," *Physical Review B* **64**, p. 195, 2001.

[9] J. Drechsel, B. Maennig, F. Kozlowski, M. Pfeiffer, K. Leo, and H. Hoppe, "Efficient organic solar cells based on a double p-i-n architecture using doped wide-gap transport layers," *Applied Physics Letters* **86**, p. 244102, 2005.

[10] V. Shrotriya, G. Li, Y. Yao, T. Moriarty, K. Emery, and Y. Yang, "Accurate measurement and characterization of organic solar cells," *Advanced Functional Materials* **16**, pp. 2016–2023, Oct. 2006.

[11] R. Schueppel, R. Timmreck, N. Allinger, T. Mueller, M. Furno, C. Uhrich, K. Leo, and M. Riede, "Controlled current matching in small molecule organic tandem solar cells using doped spacer layers," *Journal of Applied Physics* **107**(4), p. 044503, 2010.

[12] S. Pfuetzner, A. Petrich, C. Malbrich, J. Meiss, M. Koch, M. K. Riede, M. Pfeiffer, and K. Leo, "Characterisation of different hole transport materials as used in organic p-i-n solar cells," *Organic Optoelectronics and Photonics III* **6999**(1), p. 69991M, SPIE, 2008.

[13] M. M. Wienk, J. M. Kroon, W. J. H. Verhees, J. Knol, J. C. Hummelen, P. A. van Hal, and R. A. J. Janssen, "Efficient methano[70]fullerene/mdmo-ppv bulk heterojunction photovoltaic cells," *Angewandte Chemie International Edition* **42**(29), pp. 3371–3375, 2003.

[14] J. Drechsel, B. Maennig, D. Gebeyehu, M. Pfeiffer, K. Leo, and H. Hoppe, "Mip - type organic solar cells incorporating phthalocyanine/fullerene mixed layers and doped wide-gap transport layers," *Org. Electron.* (4), p. 175, 2004.

[15] S. Reineke, F. Lindner, G. Schwartz, N. Seidler, K. Walzer, B. Lussem, and K. Leo, "White organic light-emitting diodes with fluorescent tube efficiency," *Nature* **459**, pp. 234–238, May 2009.

[16] J. Drechsel, A. Petrich, M. Koch, S. Pfützner, R. Meerheim, S. Scholz, K. Walzer, M. Pfeiffer, and K. Leo, "Influence of material purification by vacuum sublimation on organic optoelectronic device performance," *SID Symposium Digest of Technical Papers* **37**, p. 1692, 2006.

[17] G. Orlandi and F. Negri, "Electronic states and transitions in c60 and c70 fullerenes," *Photochem. Photobiol. Sci.* **1**, p. 289308, 2002.

[18] W. Zhao and A. Kahn, "Charge transfer at n-doped organic-organic heterojunctions," *Journal of Applied Physics* **105**, p. 123711, June 2009.

[19] S. Pfuetzner, J. Meiss, A. Petrich, M. Riede, and K. Leo, "Improved bulk heterojunction organic solar cells employing c70 fullerenes," *Applied Physics Letters* **94**(22), p. 223307, 2009.

[20] A. J. Ikushima, T. Kanno, S. Yoshida, and A. Maeda, "Valence and conduction band edges of metal-phthalocyanines and carrier behavior," *Thin Solid Films* **273**(1-2), pp. 35 – 38, 1996. International Symposium on Ultra Materials for Picotransfer.

[21] W. Gao and A. Kahn, "Controlled p-doping of zinc phthalocyanine by coevaporation with tetrafluorotetracyanoquinodimethane: A direct and inverse photoemission study," *Appl. Phys. Lett.* **79**(24), pp. 4040–4042, 2001.

[22] B. Kippelen and J.-L. Bredas, "Organic photovoltaics.," *Energy & Environmental Science* **2**(3), pp. 251–261, 2009.